International Journal of Mining Science and Technology 33 (2023) 447–462

Contents lists available at ScienceDirect

International Journal of Mining Science and Technology

journal homepage: www.elsevier.com/locate/ijmst

A failure criterion for shale considering the anisotropy and hydration based on the shear slide failure model

Qiangui Zhang [a,b,c,*], Bowei Yao [a], Xiangyu Fan [c,d,*], Yong Li [e,*], Nicholas Fantuzzi [f], Tianshou Ma [a,c], Yufei Chen [d], Feitao Zeng [b], Xing Li [g], Lizhi Wang [a]

[a] Petroleum Engineering School, Southwest Petroleum University, Chengdu 610500, China
[b] Department of Civil, Geological and Mining Engineering, École Polytechnique de Montréal, Montreal H3T 1J4, Canada
[c] State Key Laboratory of Oil and Gas Reservoir Geology and Exploitation, Southwest Petroleum University, Chengdu 610500, China
[d] School of Geoscience and Technology, Southwest Petroleum University, Chengdu 610500, China
[e] State Key Laboratory of Coal Mine Disaster Dynamics and Control, Chongqing University, Chongqing 400030, China
[f] Department of Civil, Chemical, Environmental and Materials Engineering, University of Bologna, Bologna 40136, Italy
[g] Department of Civil and Mineral Engineering, University of Toronto, Toronto M5S 1A4, Canada

ARTICLE INFO

Article history:
Received 2 March 2022
Received in revised form 25 October 2022
Accepted 29 October 2022
Available online 3 March 2023

Keywords:
Shale
Failure criterion
Mechanical strength
Shear slide failure
Anisotropy
Hydration

ABSTRACT

A failure criterion fully considering the anisotropy and hydration of shale is essential for shale formation stability evaluation. Thus, a novel failure criterion for hydration shale is developed by using Jaeger's shear failure criterion to describe the anisotropy and using the shear strength reduction caused by clay minerals hydration to evaluate the hydration. This failure criterion is defined with four parameters in Jaeger's shear failure criterion (S_1, S_2, α and φ), three hydration parameters (k, ω_{sh} and σ_s) and two material size parameters (d and l_0). The physical meanings and determining procedures of these parameters are described. The accuracy and applicability of this failure criterion are examined using the published experimental data, showing a cohesive agreement between the predicted values and the testing results, R^2 = 0.916 and AAREP (average absolute relative error percentage) of 9.260%. The error ($|D_p|$) is then discussed considering the effects of β (angle between bedding plane versus axial loading), moisture content and confining pressure, presenting that $|D_p|$ increases when β is closer to 30°, and $|D_p|$ decreases with decreasing moisture content and with increasing confining pressure. Moreover, $|D_p|$ is demonstrated as being sensitive to S_1 and being steady with decrease in the data set when β is 0°, 30°, 45° and 90°.

1. Introduction

To accurately evaluate the stability of geotechnical engineering structures using a reasonable failure criterion is extremely crucial [1,2] because it can scientifically guide the support to ensure long-term stability [3]. Shale, a clastic sedimentary rock, has the characteristics of obvious bedding planes and high clay minerals content [4]. Therefore, the stability evaluation of shale formation is very difficult since the mechanical behaviors of shale are similar to many other rocks, complicated by water absorption [5]. Although many failure criteria have been developed for different kinds of rocks or soils considering different stress conditions [6,7], few of them are suitable for predicting the strength of hydration shale because it is challenging to consider the effects of both anisotropy and hydration. Thus, it is vital to develop a failure criterion for hydration shale, which is meant for handling the instability problems of the geotechnical engineering structure related to shale.

The mechanical properties of rocks are highly affected by water [8]. Water would weaken the bonds of the original structures inside coal, resulting in reductions in the cohesion and shear strength [9]. Thus, since water invasion cannot be avoided for many geotechnical engineering structures in natural conditions, a good failure criterion should consider the effect of water (or hydration) to predict the strength of rocks, especially for shale, which contains lots of clay minerals. Lashkaripour and Passaris [10] pointed out that, when it comes to shale strength evaluation, moisture content (ω_w) can be considered as an index, and thus, some empirical failure criteria for rocks have been developed related to ω_w afterwards [11]. As well as, some scholars modified the strength parameters in the widely accepted failure criteria to con-

* Corresponding authors.
E-mail addresses: qgzhang@swpu.edu.cn (Q. Zhang), 199931010004@swpu.edu.cn (X. Fan), yong.li@cqu.edu.cn (Y. Li).

https://doi.org/10.1016/j.ijmst.2022.10.008
2095-2686/

sider the effect of water on the rock strength. For example, Huang et al. [12] adopted the reducing cohesion and friction angle caused by hydration in Mohr-Coulomb failure criterion; Li et al. [13] gave a failure criterion using a reduction of m_i (material constant) in the Hoek-Brown failure criterion to describe the rock strength change affected by water absorption. Although people know that rock strength is highly related to water and some failure criteria were developed using ω_w to evaluate hydrated rock strength, these criteria are almost developed from empirical formula or using modified parameters in existing failure criteria. These would cause an unclear physical meaning, and they still have low accuracy in evaluating the strength of hydration shale.

The shale strength also appears to be anisotropy resulting from the shale mechanical properties, which are controlled by the weak bedding planes [14]. Therefore, the shale strength cannot be properly described by an isotropic failure criterion [15], but can be predicted by the failure criteria considering their microstructure in spatial anisotropy [16]. Therefore, some failure criteria for transversely isotropic rocks were developed to handle the stability evaluation of geotechnical engineering structures. Jaeger [17] suggested a shear failure criterion early for transversely isotropic rocks, in which the rock cohesion is assumed as variation with the angle between bedding plane versus axial loading (β), whereas the friction angle is regarded as constant. This failure criterion was then modified by Donath [18] to clearly show the relationship between the maximum and minimum principal stresses (σ_1 and σ_3), and it can predict the strength of transversely isotropic rocks well [19]. By using that the anisotropy of rock strength can be described through the orientation dependence of the parameters m and s (material constants) in Hoek-Brown failure criterion, Saroglou and Tsiambaos [20] and Zhang et al. [21] developed two modified Hoek-Brown failure criteria for predicting the strength of transversely isotropic rocks. These modified Hoek-Brown failure criteria show excellent performance in the strength prediction of rocks, but their physical meanings are missed because the Hoek-Brown failure criterion is an empirical formula [22]. Thus, some failure criteria were developed to reveal the meaning of the failure mechanism in rocks, and the representative ones include the failure criteria formulated in terms of the stress state [23] and microstructure characteristics of rocks [24]. As mentioned above, the strength prediction for transversely isotropic rocks was well performed by the failure criteria developed by the empirical formula and the formula obtained from the structural characteristics of rocks. Particularly, many failure criteria developed from the geometry of transversely isotropic rocks show clear physical meaning, indicating that the structural characteristics of rocks can be formulated to predict the strength of this kind of rock. However, these failure criteria focus on the anisotropic characteristics of rocks, and a few of them consider the water's effect.

From what has been discussed above, many failure criteria were developed for transversely isotropic rocks, and a few failure criteria were obtained for rocks after water absorption. However, few of them take account of the effects of both anisotropy and hydration. Many rocks, especially shale, have anisotropy and hydration characteristics, which can significantly affect their mechanical properties [8,14]. Thus, in the present study, a new failure criterion for hydration shale is proposed based upon Jaeger's shear failure criterion to describe the anisotropy of shale, and the effect of hydration on the shale strength is incorporated into this failure criterion by the concept that the shear strength of the slip plane would decrease for the shale after water absorption. The performance, model parameters sensibility and prediction performance with limited experimental data of the new failure criterion are then demonstrated.

2. Failure criterion for hydration shale

2.1. Failure criterion of dry shale

For the dry shale with bedding plane direction inclined at β to the direction of axial stress, the shear strength for the shale under uniaxial compression condition can be expressed as [17]:

$$S = S_1 - S_2 \cos 2(\alpha - \beta) \tag{1}$$

where S is the shear strength of a plane in the direction at α to the direction of axial stress for dry shale, MPa; S_1 and S_2 the model constants, MPa; and α the angle between the shear failure plane and the direction of axial stress (Fig. 1), (°). α is in the range between 0° to 90° and its practical range would be much smaller, for the homogeneous rocks when the failure occurs at the most vulnerable surface, and α is approximately equal to 30° [18,25].

Then, if the shear failure appears on the plane inclined at α to the direction of axial stress with a confining pressure (σ_3), the failure criterion of dry shale (Jaeger's shear failure criterion), which is a typical shear slide failure model for rocks, can be obtained, expressed as [17,18]:

$$\sigma_1 = \sigma_3 \frac{\cos\alpha(\sin\alpha + \tan\varphi\cos\alpha)}{\sin\alpha(\cos\alpha - \tan\varphi\sin\alpha)} + \frac{S_1 - S_2\cos 2(\alpha-\beta)}{\sin\alpha(\cos\alpha - \tan\varphi\sin\alpha)} \tag{2}$$

where σ_1 is the maximum principal stress (axial stress) at failure, MPa; σ_3 the minimum principal stress (confining pressure), MPa; and φ the internal friction angle of the rock matrix, (°).

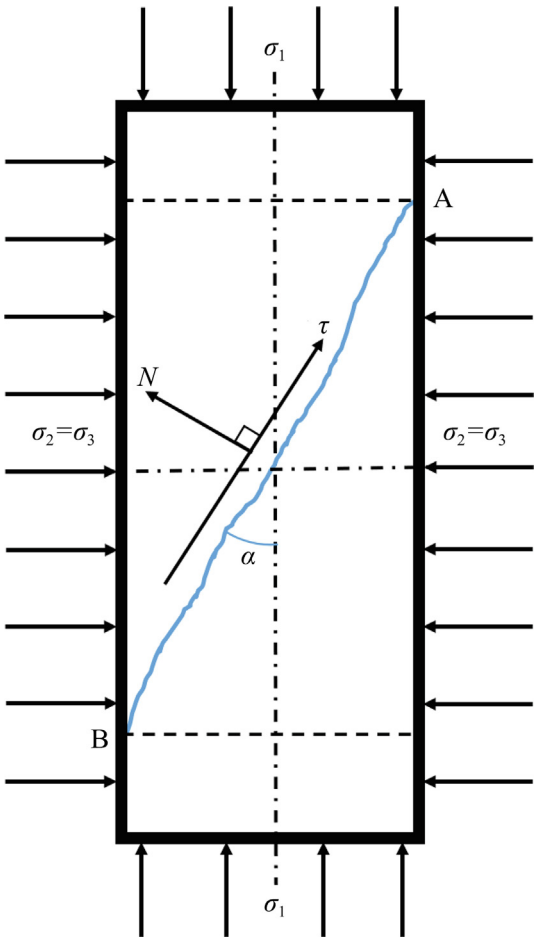

Fig. 1. Schematic diagram of the shear slide failure model of rocks. Notes: N is the normal stress, MPa; τ is the shear stress, MPa; σ_2 and σ_3 are the confining pressure, MPa.

φ is determined by the experimental data of triaxial compression tests under different σ_3 for the shale sample at β=90°, based on the concept of Jaeger's shear failure criterion. In the Jaeger's shear failure criterion, φ is a strength parameter of the shale matrix sheets, and the effect of anisotropy is determined by S_1, S_2 and β. Thus, the experimental data of the shale sample at β=90° that is used for fitting φ, is according to the following rule for the shale sample conducted by compression tests: No matter how the confining pressure is, the shear failure plane would cut the shale matrix sheets during compression tests [26]. However, for the shale sample at other β, the shear failure would happen at the bedding plane, for which condition, the strength of the bedding plane will be the major factor in determining the internal friction angle of rocks, and the data cannot be used for fitting φ.

2.2. Shear strength reduction of hydration shale

Shale hydration, which is actually clay minerals intercrystalline hydration, can alter shale microstructures resulting in the variations of Van der Waals force, double-layer repulsive force, and hydration force, the sum of which is the total force in two charged parallel plates [27]. The smaller distance between intercrystalline layers will lead the short-range repulsive effect of hydration force to become more dominant [28]. Thus, a strong hydration swelling stress will appear to make the distance between intercrystalline layers increase [27], and this process would cause the Van der Waals force in two charged parallel plates to be highly reduced. Finally, the total force in two charged parallel plates of shale may reduce after hydration. Here, we use a shear strength reduction (σ_s) of the direct shear plane in shale resulting from the total force decrease after clay minerals intercrystalline hydration to determine the strength decrease of hydration shale. σ_s can be obtained by two direct shear tests using the dry shale sample and saturated hydration shale, expressed as Eq. (3), and the shear plane of these direct shear tests should be the clay minerals layer.

$$\sigma_s = \sigma_{ds} - \sigma_{hs} \tag{3}$$

where σ_{ds} is the shear strength of the direct shear plane for the dry shale when the shear failure is along the single clay minerals layer, MPa; and σ_{hs} the shear strength of the direct shear plane for the saturated hydration shale when the shear failure is along the single saturated hydration clay minerals layer, MPa.

2.3. Failure criterion of saturated hydration shale

For saturated hydration shale, the shale failure is assumed as in the hydrated clay minerals layer based on the test result by Fan et al. [29]. Thus, the shear strength reduction ($\sigma_{s\beta}$) of shale concerning β is suggested to determine the strength change of shale caused by the saturated hydration of shale compared with the dry shale. Therefore, the shear strength (S') of a plane in the direction at α to the direction of axial stress for the saturated hydration shale should be:

$$S' = S - \sigma_{s\beta} \tag{4}$$

Combining Eqs. (1) and (4), the failure criterion of saturated hydration shale under uniaxial compression condition can be expressed as:

$$S' = S_1 - S_2 \cos 2(\alpha - \beta) - \sigma_{s\beta} \tag{5}$$

Thus, the failure criterion of saturated hydration shale under a confining pressure (σ_3) can be obtained by combining Eqs. (2) and (5), as shown by Eq. (6).

$$\sigma_1 = \sigma_3 \frac{\cos\alpha(\sin\alpha + \tan\varphi\cos\alpha)}{\sin\alpha(\cos\alpha - \tan\varphi\sin\alpha)} + \frac{S_1 - S_2\cos 2(\beta - \alpha)}{\sin\alpha(\cos\alpha - \tan\varphi\sin\alpha)} - \frac{\sigma_{s\beta}}{\sin\alpha(\cos\alpha - \tan\varphi\sin\alpha)} \tag{6}$$

As shown in Fig. 2a, AB is the shear failure plane of homogeneous rock. Considering the shear strength reduction (σ_s) in the clay minerals layer caused by the hydration of shale, a reduced angle between the hydrated clay minerals layer and AB (θ) will cause an increased effect of hydrated clay minerals layers on the shale strength when the shear failure is along AB. Hence, the shear strength reduction ($\sigma_{s\beta}$) will be greater for the hydration shale. However, it is tough to determine $\sigma_{s\beta}$ by θ and σ_s. Here we use the product of the number of the saturated hydration clay minerals layers which are across the normal (OP) of AB in the shale sample (m) and σ_s to determine $\sigma_{s\beta}$, as shown in Eq. (7). This is based on the rule of that the lower θ is, the higher m will be, as shown in Fig. 2. In addition, σ_s is determined by direct shear tests and $\sigma_{s\beta}$ is used to evaluate the strength reduction caused by shale hydration for compression tests, the product of m and σ_s is thus not equal to $\sigma_{s\beta}$ due to the differences in test methods, size and material of shale sample. Therefore, k is employed here to correct their differences.

$$\sigma_{s\beta} = km\sigma_s \tag{7}$$

where k is the coefficient for correcting the differences in test method, size, and material of shale sample, dimensionless; and m the number of the saturated hydration clay minerals layers across the normal (OP) of AB in the shale sample, integer.

As shown in Fig. 2a, m can be obtained by counting the number of clay minerals layers which are across MO, expressed as:

$$m = \frac{d\cos(\alpha - \beta)}{l_0\cos\alpha} \tag{8}$$

where d is the shale sample diameter, mm; and l_0 the thickness of one alternant clay minerals layer and rock matrix layer, mm, as shown in Fig. 2b.

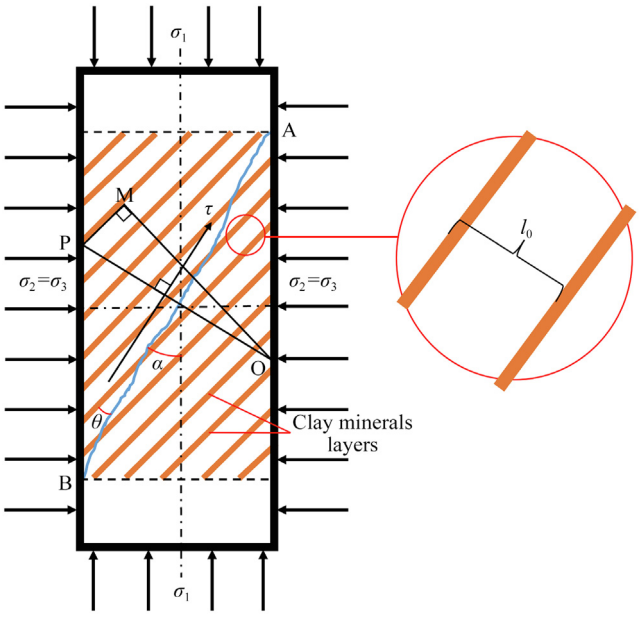

(a) Relationship between bedding planes and the shear failure plane of the homogeneous rock (b) Thickness of one alternant clay minerals layer and rock matrix layer (l_0)

Fig. 2. Schematic diagram for determining the shear strength reduction of saturated hydration shale.

Thus, $\sigma_{s\beta}$ can be obtained by substituting Eq. (8) into Eq. (7), expressed as:

$$\sigma_{s\beta} = \frac{kd\cos(\alpha-\beta)}{l_0\cos\alpha}\sigma_s \tag{9}$$

Finally, the failure criterion of saturated hydration shale can be obtained by substituting Eq. (9) into Eq. (6), expressed as:

$$\begin{aligned}\sigma_1 = {} & \sigma_3\frac{\cos\alpha(\sin\alpha+\tan\varphi\cos\alpha)}{\sin\alpha(\cos\alpha-\tan\varphi\sin\alpha)} \\ & + \frac{S_1 - S_2\cos 2(\alpha-\beta)}{\sin\alpha(\cos\alpha-\tan\varphi\sin\alpha)} \\ & - \frac{kd\sigma_s\cos(\alpha-\beta)}{l_0\sin\alpha\cos\alpha(\cos\alpha-\tan\varphi\sin\alpha)}\end{aligned} \tag{10}$$

2.4. Failure criterion of unsaturated hydration shale

For unsaturated hydration shale, the shear strength reduction ($\sigma_{u\beta}$) of the clay minerals layer due to the unsaturated hydration of shale is assumed to be in direct proportion to moisture content (ω_w), which is similar to other rocks [30,31]. Thus, $\sigma_{u\beta}$ can be expressed as:

$$\sigma_{u\beta} = \sigma_{s\beta}\frac{\omega_w}{\omega_{sh}} \tag{11}$$

where ω_{sh} is the moisture content of saturated hydration shale, %.

Therefore, using $\sigma_{u\beta}$ to replace $\sigma_{s\beta}$, the failure criterion of unsaturated hydration shale can be obtained by combining Eqs. (6), (9), and (11), expressed as:

$$\begin{aligned}\sigma_1 = {} & \sigma_3\frac{\cos\alpha(\sin\alpha+\tan\varphi\cos\alpha)}{\sin\alpha(\cos\alpha-\tan\varphi\sin\alpha)} \\ & + \frac{S_1 - S_2\cos 2(\beta-\alpha)}{\sin\alpha(\cos\alpha-\tan\varphi\sin\alpha)} \\ & - \frac{kd\omega_w\sigma_s\cos(\alpha-\beta)}{l_0\omega_{sh}\sin\alpha\cos\alpha(\cos\alpha-\tan\varphi\sin\alpha)}\end{aligned} \tag{12}$$

3. Parameters determination method

The proposed failure criterion, a nine-parameter model, is developed from Jaeger's shear failure criterion for transversely isotropic rocks, using the shear strength reduction of hydration shale and the geometrical relationship between the hydrated clay minerals layers and the shear failure plane to consider the effect of shale hydration. Thus, the nine parameters of the proposed failure criterion can be categorized into three groups: (1) Strength parameters of Jaeger's shear failure criterion: S_1, S_2, α and φ; (2) Hydration parameters of shale: σ_s, k and ω_{sh}; (3) Material size parameters: d and l_0.

3.1. Determination method of S_1, S_2, α and φ

α is set as 30° as mentioned in Section 2.1. S_1 and S_2 are determined by fitting the uniaxial compression test data for the dry shale samples at different β, using Eq. (2). φ is determined by fitting the triaxial compression test data for shale samples at β=90°, at least four confining pressures, using Eq. (2).

3.2. Determination method of σ_s, k and ω_{sh}

As mentioned in Section 2.2, σ_s can be obtained using two direct shear tests for the dry shale sample and saturated hydration shale. The test procedure is presented as follows: first, two shale samples (diameter of 50.8 mm, height of 25.4 mm, or other size requested by direct shear test standard, the effect of size difference can be corrected by k) are prepared for the direct shear tests, and one is dried in an incubator at a temperature of 105 ℃ for 24 h and the other one is saturated with fresh water using the vacuum saturation test according to the "Regulation for testing the physical and mechanical properties of rock—Part 5: Test for determining the water absorption of rock". These two shale samples then undergo the direct shear tests according to the "Regulation for testing the physical and mechanical properties of rock—Part 28: Test for determining the strength of rock mass (Direct shear test)", and the shear strengths of the direct shear planes for the dry shale and the saturated hydration shale, when the shear failure is along the single clay minerals layer (σ_{ds} and σ_{hs}), can be obtained by dividing the peak shear force by the cross-sectional area of the shale samples. Finally, σ_s can be calculated using Eq. (3).

k can be determined by fitting the compression test data for shale samples at β=90°, with any level of moisture content (ω_w) and confining pressure (σ_3), using Eq. (12).

Saturated hydration shale involves the amount of free water in pores and water in hydrated clay minerals. Thus, ω_{sh} should be determined by the saturated shale sample for compression test. Since shale is usually tight and has low porosity, we use a test method of injecting water into a vacuum shale sample with positive pressure to determine ω_{sh}. The test procedure is presented as follows: First, a shale sample (diameter of 25.4 mm, height of 50.8 mm) is prepared. Second, this shale sample is dried in an incubator with a temperature of 105 ℃ for 24 h, and its weight is then measured as M_d. Third, this shale sample is put into a pressure vessel, and the air in the shale sample is pumped out by a vacuum pump. Fourth, a confining pressure of 10 MPa is applied to the shale sample. Fifth, water is injected into the shale sample from one side by a positive pressure of 8 MPa until the water can be seen on the other side of the shale sample for at least 24 h. Finally, the shale sample is taken out and is then measured as M_w. Thus, ω_{sh} can be calculated by Eq. (13).

$$\omega_{sh} = \frac{M_w - M_d}{M_d}\times 100\% \tag{13}$$

3.3. Determination method of d and l_0

d is the diameter of the shale sample, which can be measured directly using a vernier caliper. l_0 is the thickness of one alternant clay minerals layer and rock matrix layer, which can be measured directly by the digital image of an electron microscope for bedding planes section of shale.

4. Evaluation of the proposed failure criterion

4.1. Mechanical behavior of hydration shale and database for evaluation

The data for demonstrating the proposed failure criterion is collected from the literature of Zhang et al. [32,33]. The shale samples with seven bedding plane orientations (β, in degrees) relative to the axial direction were drilled from one shale outcrop collected from the Silurian Longmaxi formation in Shuanghe Town, Changning County, Sichuan Province, Southwest China. The shale samples were then prepared with three moisture contents: dry shale samples (S-level moisture content), L-level moisture content (ω_w=0.594%–0.753% with an average value of 0.674%) and H-level moisture content (ω_w=0.909%–1.127% with an average value of 1.020%). The confining pressures of these compression tests were set as 0, 10, 20 and 30 MPa.

4.1.1. Stress-strain curves

Fig. 3 presents the stress-strain curves of the shale samples under a confining pressure of 10 MPa. The shale samples all have a significant elastic deformation stage, short plastic deformation stage and no compaction deformation stage, and the stress drops very quickly during the residual stress stage. These indicate that the shale is characterized by brittleness [34]. In addition, the mechanical behaviors of the shale samples are highly dependent on β, ω_w and σ_3, and their detailed presentation can be seen in the literature of Zhang et al. [32]. From Fig. 3, we can infer that the clay minerals hydration alone bedding plane would make the failure of shale samples prefers alone the hydrated bedding plane resulting in reduced mechanical behaviors of the hydration shale samples. Therefore, the shale samples would fail as a shear slide failure mode coupling the effects of hydration, bedding plane and confining pressure, as shown in Fig. 4. This indicates that the basal concept for developing the new failure criterion can match the real failure mode of shale samples very well.

The symbol S, L, and H indicate the dry shale sample, hydration shale sample with low and high moisture contents, respectively; ε_{3C} is the radial strain calculated using the displacement of the circumferential extensometer, %; ε_{VC} is the volumetric strain calculated using the displacement of the circumferential extensometer, %; and ε_1 is the axial strain, %.

The broken red lines indicate the main shear failure mode; the broken white lines indicate the other failure features affected by bedding plane or microcracks.

4.1.2. Data for evaluating the proposed failure criterion

The 74 samples compression tests' data all [32], as shown in Fig. 3, indicate that the shale samples collected from Longmaxi formation exhibit strong anisotropy [35], showing the lowest strength occurs for the shale sample at β=30°. Moreover, the hydration shale sample would have smaller strength than the dry one. The strength change rules of the shale samples with β and ω_w highly match the concept for developing the new failure criterion. Using these data, the performances of the proposed failure criterion are evaluated as shown in Sections 4.5–4.7.

4.2. Other failure criteria used for comparison

We briefly present four widely accepted failure criteria for comparison: Cai-Huang criterion, modified Hoek–Brown criterion, Saeidi criterion and Al-Bazali criterion. The details of these failure criteria are introduced as follows.

4.2.1. Cai-Huang criterion

Cai-Huang criterion has considered the effects of both hydration and bedding planes on rock strength. It is developed by the concept of two failure modes in rock: failure of the dry rock matrix and failure of dry weak planes in rock, expressed as Eq. (14) [36].

$$\begin{cases} \sigma_1 = \sigma_3 + \frac{2(C_w+\sigma_3\tan\varphi_w)}{(1-\tan\varphi_w\cot\beta)\sin 2\beta} \quad (\beta_1 \leqslant \beta \leqslant \beta_2) \\ \sigma_1 = \frac{1+\sin\varphi_0}{1-\sin\varphi_0}\sigma_3 + \frac{2C_0\cos\varphi_0}{1-\sin\varphi_0} \quad (\beta < \beta_1 \ or \ \beta > \beta_2) \\ \beta_1 = \frac{\varphi_w}{2} + \frac{1}{2}\arcsin\frac{(\sigma_1+\sigma_3+2C_w\cot\varphi_w)\sin\varphi_w}{\sigma_1-\sigma_3} \\ \beta_2 = \frac{\pi}{2} + \frac{\varphi_w}{2} - \frac{1}{2}\arcsin\frac{(\sigma_1+\sigma_3+2C_w\cot\varphi_w)\sin\varphi_w}{\sigma_1-\sigma_3} \end{cases} \tag{14}$$

where β_1 and β_2 are the specific angles among β distinguishing failure along or across weak planes of shale, (°); C_0 the cohesion of dry rock matrix, MPa; φ_0 the internal friction angle of dry rock matrix, (°); C_w the cohesion of weak planes in dry rock, MPa; and φ_w the internal friction angle of weak planes in dry rock, (°).

The method of reducing cohesion and internal friction angle is used to describe the hydration effect, and the expressions of the cohesion and the internal friction angle for rock after water absorption are given by Huang et al. [12]:

$$\begin{cases} C_0[\omega_w] = C_0 - a_1\omega_w \\ \varphi_0[\omega_w] = \varphi_0 - b_1\omega_w \\ C_w[\omega_w] = C_w - a_2\omega_w \\ \varphi_w[\omega_w] = \varphi_w - b_2\omega_w \end{cases} \tag{15}$$

where $C_0[\omega_w]$ is the cohesion of rock matrix changed with ω_w, MPa; $\varphi_0[\omega_w]$ the internal friction angle of rock matrix changed with ω_w, (°); $C_w[\omega_w]$ the cohesion of weak planes of rock changed with ω_w, MPa; $\varphi_w[\omega_w]$ the internal friction angle of weak planes of rock changed with ω_w, %; and a_1, a_2, b_1 and b_2 the model parameters, dimensionless.

Therefore, using $C_0[\omega_w]$, $\varphi_0[\omega_w]$, $C_w[\omega_w]$, and $\varphi_w[\omega_w]$ in Eq. (15) to take the place of C_0, φ_0, C_w and φ_w in Eq. (14), the strength of hydration shale can be predicted by Eq. (14).

4.2.2. Modified Hoek-Brown criterion

The modified Hoek-Brown criterion has the capacity for predicting the strength of transversely isotropic rocks. This failure criterion was developed from Hoek-Brown criterion [22] by using a parameter k_β to describe the anisotropy of rocks, expressed as [20]:

$$\sigma_1 = \sigma_3 + \sigma_{c\beta}\left(k_\beta m_i\frac{\sigma_3}{\sigma_{c\beta}} + 1\right)^{0.5} \tag{16}$$

where k_β is the model parameter describing the anisotropy effect on rock strength, dimensionless; m_i the material constant, dimension-

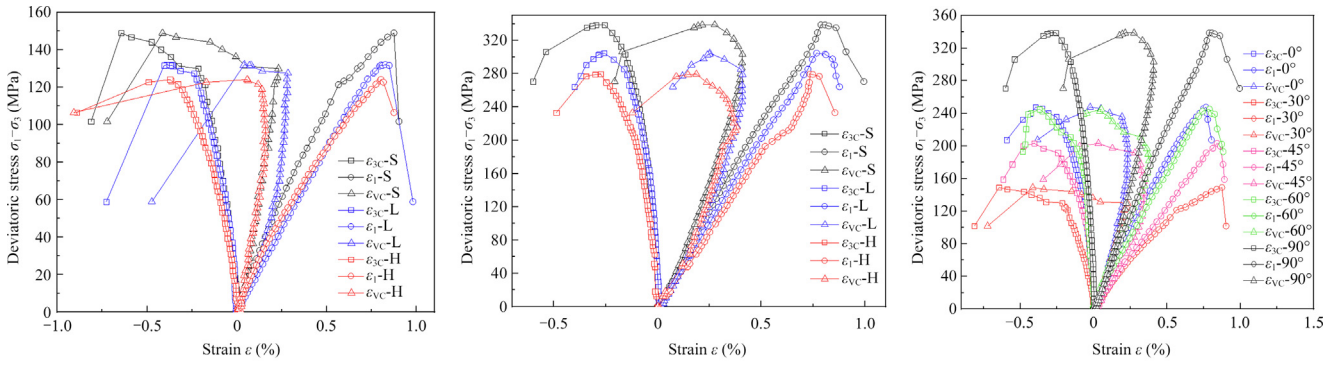

(a) The shale samples with different moisture contents for β=30°

(b) The shale samples with different moisture contents for β=90°

(c) The dry shale samples for β of 0°, 30°, 45°, 60°, and 90°

Fig. 3. Stress-strain curves of the shale samples with different moisture contents tested under a confining pressure of 10 MPa [32,33].

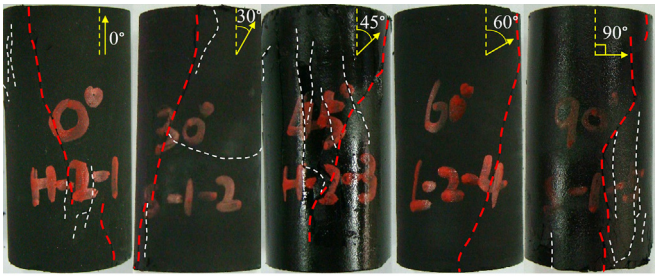

(a) β=0° (b) β=30° (c) β=45° (d) β=60° (e) β=90°

Fig. 4. Typical failure modes of the shale samples after triaxial compression tests.

less; and $\sigma_{c\beta}$ the uniaxial compressive strength at orientation β, MPa, which can be calculated by Eq. (17) [18].

$$\sigma_{c\beta} = A - D\cos 2(\beta - \beta_{min}) \tag{17}$$

where β_{min} is the angle between bedding plane versus axial loading of the rock sample having the minimum uniaxial compressive strength, (°); and A and D the model parameters, MPa.

4.2.3. Saeidi criterion

Saeidi criterion, which is a failure criterion for transversely isotropic rocks, was developed based on an empirical failure criterion introduced by Rafiai [37], expressed as [38]:

$$\sigma_1 = \sigma_3 + \sigma_{c\beta}\left(\frac{1 + A_\beta(\sigma_3/\sigma_{c\beta})}{\lambda + B_\beta(\sigma_3/\sigma_{c\beta})}\right) \tag{18}$$

where λ is the strength reduction parameter related to the rock anisotropy, dimensionless; and A_β and B_β the model parameters, dimensionless. $\sigma_{c\beta}$ can be determined by Eq. (17).

4.2.4. Al-Bazali criterion

Al-Bazali et al. [11] summarized a failure criterion of uniaxial compression condition for hydration rock, and the expression of this failure criterion is as follows:

$$\sigma_c = \sigma_c^{dry}\exp(A_u\omega_w) \tag{19}$$

where σ_c is the uniaxial compressive strength of rock after water absorption, MPa; A_u the model parameter, dimensionless; and σ_c^{dry} the uniaxial compressive strength of dry rock, MPa.

4.3. Prediction performance indicators

We use three different error measurements to assess the validity of the proposed failure criterion: the regression R-square value (R^2), the discrepancy percentage (D_p), and the average absolute relative error percentage (AAREP). Their expressions are given by [39]:

$$R^2 = 1 - \frac{\sum_{i=1}^{n}\left(\sigma_{1,i}^{test} - \sigma_{1,i}^{pred}\right)^2}{\sum_{i=1}^{n}\left(\sigma_{1,i}^{test} - E\left[\sigma_{1,i}^{test}\right]\right)^2} \tag{20}$$

$$D_{p,i} = \frac{\sigma_{1,i}^{pred} - \sigma_{1,i}^{test}}{\sigma_{1,i}^{test}} \times 100\% \tag{21}$$

$$AAREP = \frac{\sum_{i=1}^{n}|D_{p,i}|}{n} \tag{22}$$

where n is the number of available observations; σ_1^{test} the tested maximum principal stress (axial stress) at failure, MPa; σ_1^{pred} the maximum principal stress (axial stress) at failure predicted by the criteria, MPa; and $E[\cdot]$ the expected (or statistical mean) operator.

4.4. Parameters of the failure criteria

4.4.1. Parameters of the proposed failure criterion

The parameters of the proposed failure criterion are determined according to the method mentioned in Section 3. Using the experimental data presented in Section 4.1, S_1, S_2 and φ are obtained by fitting the uniaxial compression test data for the dry shale samples at β=0°, 15°, 30°, 45°, 60°, 75° and 90°, and the triaxial compression test data for the shale samples at β=90° under the confining pressures of 0, 10, 20, and 30 MPa, using Eq. (2). α is set as 30° according to the works presented in the literatures of Donath [18] and Chen et al. [25], as mentioned in Section 2.1.

ω_{sh} is determined by the test method of injecting water into a vacuum sample with a positive pressure as introduced in Section 3.2, and M_d and M_w are measured as 64.994 and 66.703 g, respectively, for the shale sample with a diameter of 25.52 mm and height of 49.97 mm, so ω_{sh} can be determined as 1.120% using Eq. (13). σ_s is obtained by two direct shear tests for the dry shale sample with a diameter of 50.01 mm and height of 25.67 mm and the saturated hydration shale sample with a diameter of 49.98 mm and height of 25.54 mm, following the test procedure as introduced in Section 3.2. Fig. 5 presents the rock direct shear device (Fig. 5a), the saturated shale sample (Fig. 5b) and the dry shale sample (Fig. 5c) after the direct shear tests. As shown in Fig. 5b and c, the shear failure planes of the two shale samples are along the bedding planes of shale, and a hydrated crack can be clearly seen in the saturated shale sample. σ_{ds} and σ_{hs} are measured as 1.58 and 0.32 MPa, respectively, and σ_s is therefore calculated as 1.26 MPa by Eq. (3). k is determined as 5.720×10^{-4} by fitting the triaxial tests data for the dry shale sample and hydration shale sample with H-level moisture content at β=90° under a confining pressure of 10 MPa, using Eq. (12).

d is measured as an average value of 25.4 mm directly using a vernier caliper. l_0 is measured to be 1.978×10^{-3} mm using the digital image of an electron microscope for the bedding planes section of shale, as shown in Fig. 6.

Although some parameters are fitted by the experimental data, as mentioned above, these experimental data are very limited. Thus, the predicted values for the other shale samples with different β, moisture contents and confining pressures can be compared with the corresponding experimental data to demonstrate the proposed criterion's predictive capabilities.

The parameters of the proposed failure criterion are listed in Table 1.

4.4.2. Parameters of the other failure criteria

The parameters of the Cai-Huang criterion are determined by fitting the experimental data of the shale samples at β=30° and 90°, with S-, L-, and H-level moisture contents and confining pressures of 0, 10, 20, and 30 MPa. The parameters of the Cai-Huang criterion are presented in Table 2.

The parameters of the modified Hoek-Brown criterion are determined according to the method introduced by the literature of Saroglou and Tsiambaos [20], using the data of the dry shale samples for β=90° under the confining pressures of 10, 20, and 30 MPa and for different β under the confining pressures of 0 and 10 MPa. The parameters of the modified Hoek-Brown criterion are presented in Table 3.

A and D for calculating $\sigma_{c\beta}$ in the Saeidi criterion are determined as the same for the modified Hoek–Brown criterion and their values are shown in Table 3. λ, A_β and B_β in the Saeidi criterion are determined according to the method introduced by the literature of Saeidi et al [38], using the data of dry shale samples for different

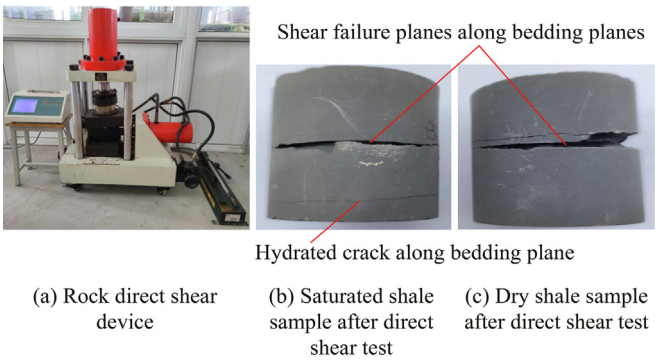

Fig. 5. Device and shale samples of direct shear tests to determine σ_s.

β tested under different confining pressures. λ, A_β and B_β are presented in Table 4.

A_u in Al-Bazali criterion is determined as −0.266 with R^2=0.956 by fitting the uniaxial compressive strength of S- and L-level moisture content shale samples. The tested σ_c^{dry} is used to calculate σ_c of the shale samples with different ω_w for the corresponding β.

4.5. Prediction performance of the proposed failure criterion

4.5.1. Comparison of the prediction performances for the failure criteria

The comparisons of the predicted σ_1 for the failure criteria with the tested results are presented in Fig. 7. For strength prediction of dry shale sample, the prediction performance of the proposed failure criterion is a little worse than that of the modified Hoek-Brown criterion, and slightly better than that of Saeidi criterion, as shown in Fig. 7a, e and f. This would be due to that the Hoek-Brown criterion can have good adaptability by adjusting the parameters (σ_{ci}, m_i and s) [20]. In addition, k_β in the modified Hoek-Brown criterion is fitted by the tested results of the shale samples for corresponding β, which implies that this criterion has high limitation due to that it cannot predict the strength for the shale sample without the tested data of the shale sample for the corresponding β. On the other hand, although the parameters (A_β, B_β and λ) in the Saeidi criterion are fitted using the tested data of the shale sample for the corresponding β, its performance is worse than the modified Hoek–Brown criterion and the proposed failure criterion. Furthermore, the modified Hoek-Brown criterion and the Saeidi criterion do not consider the effect of shale hydration, thus the proposed failure criterion shows a better performance than the two failure criteria.

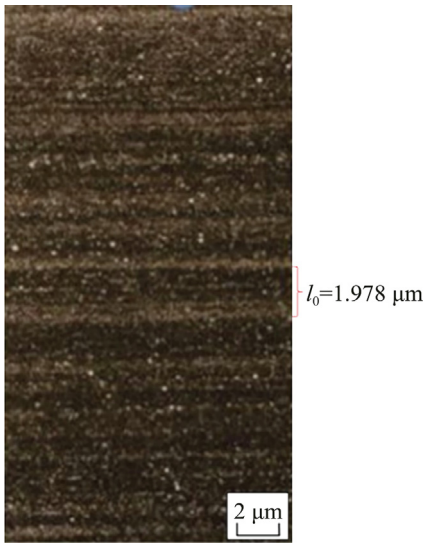

Fig. 6. Digital image of electron microscope for bedding planes section of shale.

Table 1
Parameters of the proposed failure criterion.

Parameter type	Parameter	Value
Parameters of Jaeger's shear failure criterion	S_1 (MPa)	40.439
	S_2 (MPa)	16.984
	α (°)	30
	φ (°)	44.53
Hydration parameters	k	5.720×10^{-4}
	ω_{sh} (%)	1.120
	σ_s (MPa)	1.26
Material size parameters	d (mm)	25.4
	l_0 (mm)	1.978×10^{-3}

For strength prediction of shale sample after water absorption, the prediction performance of the Al-Bazali criterion is a little better than that of the proposed failure criterion, as shown in Fig. 7b and g. However, the Al-Bazali criterion just has the capacity for predicting the rock strength under uniaxial compression condition and the parameter (A_u) is determined by fitting the tested data for the corresponding β. As well as, the tested σ_1 of the dry shale sample is used to calculate the strength of the shale sample after water absorption with the same β. These indicate that the application of the Al-Bazali criterion is highly limited.

The results of all the shale samples predicted by the proposed failure criterion agree well with the tested results, showing that R^2=0.916 and AAREP=9.260% (Fig. 7c). The error analysis of the results predicted by the Cai-Huang criterion shows that R^2 and AAREP are 0.449% and 17.821% (Fig. 7d), respectively. This indicates that the prediction performance of the proposed failure criterion is significantly better than that of the Cai-Huang criterion.

Therefore, the proposed failure criterion is generally better than the other four criteria, comprehensively considering the adaptability, the physical meaning of their parameters and the prediction accuracy of the results.

4.5.2. Prediction performance of the proposed failure criterion with the changes of β, ω_w and σ_3

Figs. 8–10 show the comparisons between the predicted values and the tested results with the changes of β, ω_w, and σ_3. Fig. 11 shows the error ($|D_p|$) of the results predicted by the proposed failure criterion compared with the tested results. As shown in Fig. 8, the predicted results and tested values both appear that σ_1 reduces with increasing β when β<30° and then increases, forming a "U" shape between σ_1 and β, which is also well agreed with the results obtained by other scholars [40,41]. As shown in Fig. 11a, the average $|D_p|$ shows higher values of the shale samples at β=15°, β=30°and β=45°, these $|D_p|$ are all bigger than 10%. According to the determination method of the parameters in the proposed failure criterion, as mentioned in Section 3.1, the experimental data of the shale samples at β=90° are used to determine φ, indicating the failure of the rock matrix layer. The sheal failure of the shale sample when β is closer to 0° and 90° is regarded as damage to the rock matrix layer [42]. In this case, we can obtain better predicted results when β is closer to 0° or 90°. At β=15°, 30° and 45°, the failures of shale samples always result from the damage to rock matrix sheets and bedding planes, and even almost result from the damage of bedding planes of the shale samples for 30°<β<45° [32]. This would cause the tested results to have poor regularity due to the complex effects of pore water, such as clay minerals

Table 2
Parameters of the Cai-Huang criterion.

Moisture content level	C_0 (MPa)	φ_0 (°)	C_w (MPa)	φ_w (°)	β_1 (°)	β_2 (°)	a_1	a_2	b_1	b_2
S	48.080	44.530	23.680	47.100	20.430	65.410	6.463	3.536	2.689	9.374
L	43.737	42.723	21.304	40.801	20.430	65.410	6.463	3.536	2.689	9.374
H	41.501	41.792	20.081	37.558	20.430	65.410	6.463	3.536	2.689	9.374
R^2							0.797	0.717	0.990	0.952

Table 3
Parameters of the modified Hoek-Brown criterion.

β (°)	k_β	R^2	A (MPa)	D (MPa)	R^2
0	1.451	0.999	200.96	89.12	0.872
15	1.525	0.986	200.96	89.12	0.872
30	0.709	0.936	200.96	89.12	0.872
45	0.981	0.977	200.96	89.12	0.872
60	0.861	0.846	200.96	89.12	0.872
75	0.909	0.974	200.96	89.12	0.872
90	1.000	0.950	200.96	89.12	0.872

Table 4
Parameters of the Saeidi criterion.

β (°)	A_β	B_β	λ	R^2
0	12.718	2.780	1.032	0.871
15	15.529	3.638	1.052	0.765
30	7.086	0.938	1.195	0.849
45	10.789	3.628	0.914	0.841
60	6.989	2.394	0.792	0.899
75	19.852	9.395	0.886	0.847
90	18.523	6.972	1.057	0.936

hydration, pore water pressure, water lubrication action, etc [32]. Therefore, a higher $|D_p|$ can be found for the shale samples at β=15°, 30° and 45° with higher ω_w, as shown in Fig. 8.

$|D_p|$ also varies with ω_w. As shown in Figs. 9 and 11b, the error of the predicted results rises with increasing ω_w, which is verified by the average $|D_p|$ of 7.95% for dry shale samples (S-samples), 9.69% for low-level moisture content samples (L-samples) and 10.22% for high-level moisture content samples (H-samples). This may be because of that the proposed failure criterion is a little difficult to evaluate the strength when β is closer to 30° due to the complex effects of pore water as mentioned above. As shown in Fig. 9, $|D_p|$ is slightly higher for the hydration shale sample for which β=30° compared with the $|D_p|$ for the hydration shale samples at other β. However, the tested results and the predicted values decrease with increasing ω_w, showing good consistency of the changing trend for them, and all the average $|D_p|$ are almost less than 10%. These indicate that the proposed failure criterion has a good performance for predicting the strength of hydration shale.

Fig. 10 shows a good consistency of the changes in the predicted values and the tested results with the increase in confining pressure (σ_3). The average $|D_p|$ generally decreases with the increase in σ_3, as shown in Fig. 11c, presenting that the prediction performance of the proposed failure criterion would increase with increasing σ_3. This may be due to that confining pressure can weaken the complex effects of pore water [32].

In general, $|D_p|$ is lower than 15%, with an average value of 9.260% for all the predicted results (Figs. 7 and 11), indicating that the proposed failure criterion has good performance for predicting shale strength.

4.6. Parametric sensitivity analysis of the proposed failure criterion

A sensitivity analysis of the fitting parameters is presented here. The proposed failure criterion contains nine parameters. α is set as 30° as mentioned in Section 4.4.1. φ, ω_{sh}, σ_s, d and l_0, which are the parameters of the material's inherent properties, and can be directly measured using the methods as introduced in Section 3. We analyze the three fitting parameters S_1, S_2 and k to check how the predicted results will change if these poorly accurate parameters are used. The other parameters (φ, α, ω_{sh}, σ_s, d and l_0) are invariable, as listed in Table 1, and by setting 20% growth of S_1, S_2, and k, the predicted σ_1 and its changing rate are calculated for sensitivity analysis.

Fig. 12 shows the sensitivity analysis results of S_1 and S_2. ω_w of the shale samples is set as 1%. The predicted σ_1 and its changing rate grow with increasing S_1, due to that the predicted σ_1 is positively correlated with S_1, as shown in Eq. (12). The predicted σ_1 with a 2.0 growth ratio of S_1 has changing rates of 40.752%, 45.203% and 33.791% for the shale samples at β=0°, 30°, and 90°, respectively. This implies that the predicted σ_1 is more sensitive with S_1 for the shale sample at β=30° compared with the shale samples at other β. This is because of that the minimum σ_1 (the denominator used for calculating changing rate) is predicted by the proposed failure criterion for the shale sample at β=30°, but, as shown in Eq. (12), the changed values of σ_1 ($\Delta\sigma_1$, the numerator used for calculating changing rate) are constant caused by the increasing S_1 for all β. On the other hand, the predicted σ_1 and its changing rate decrease with increasing S_2 for shale samples at β=0° and 30°, but grow with increasing S_2 for shale sample at β=90°. This is because of the predicted σ_1 that is negatively correlated with S_2 for shale samples at β=0° and 30° and is positively correlated with S_2 for the shale samples at β=90°, as shown in Eq. (12). Identical to the sensitivity analysis result for S_1, the predicted σ_1 is more sensitive with S_2 for the shale sample at β=30° too, certified by the increasing rates of the predicted σ_1 with a 2.0 growth ratio of S_2, −16.883%, −53.014% and 9.676% for the shale samples at β=0°, 30°, and 90°, respectively, as shown in Fig. 12. Besides that the minimum σ_1 is predicted by the proposed failure criterion for the shale sample at β=30°, the changed values of σ_1 ($\Delta\sigma_1$) is caused most significantly by the increasing S_2 for the shale sample at β=30°, due to that effect of S_2 on the predicted σ_1 is multiplied by $\cos2(\alpha-\beta)$. Therefore, the error of the predicted results will increase when the fitting accuracy of S_1 and S_2 reduces, and this error increase would also increase for the shale sample when β is closer to 30°. This would be one reason why $|D_p|$ is a little higher for the shale sample when β is closer to 30°, as shown in Fig. 11a.

Fig. 13 shows the sensitivity analysis results of k. The predicted σ_1 at different β, with different ω_w decreases with increasing k due to the predicted σ_1 that is negative correlated

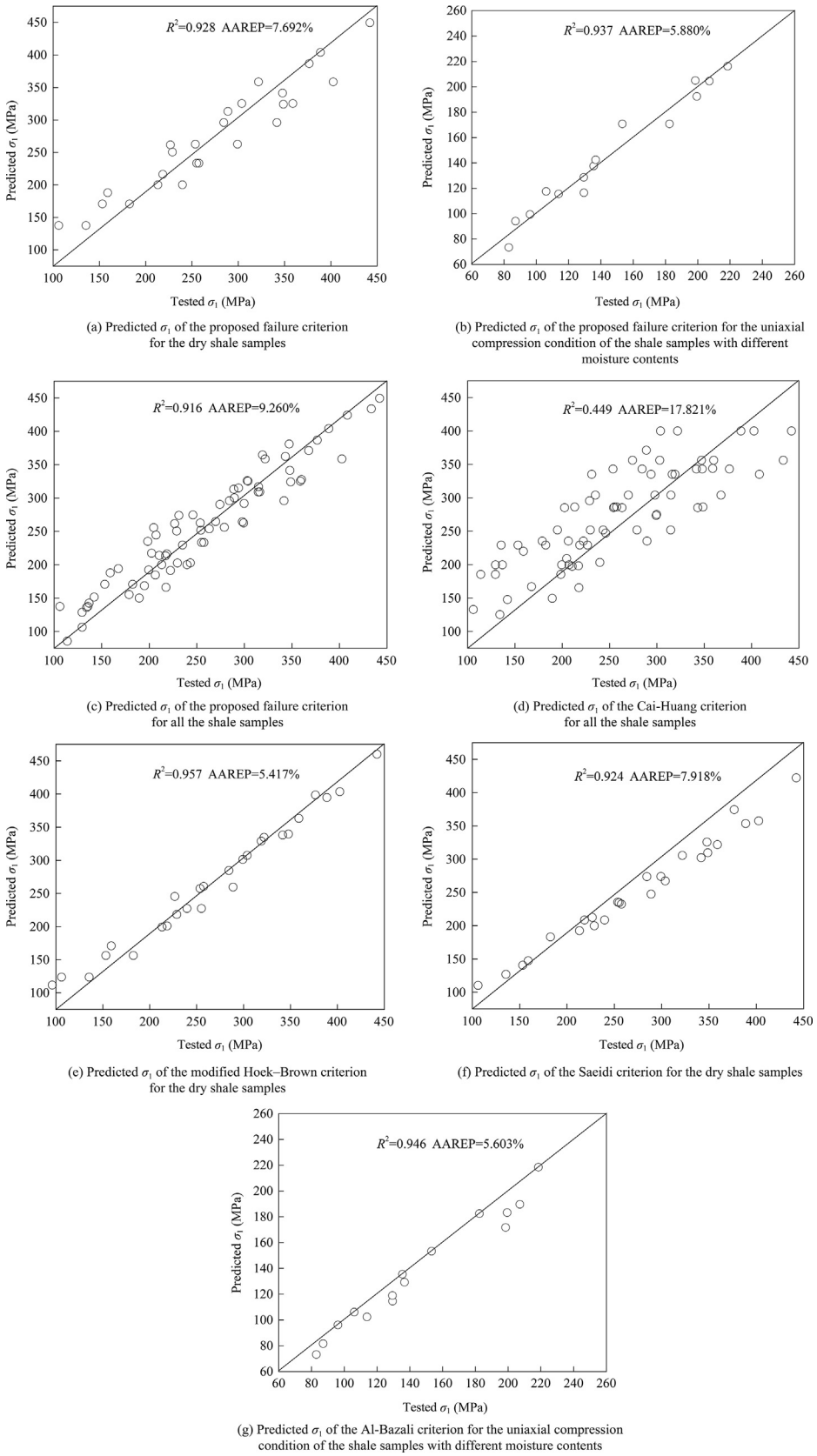

(a) Predicted σ_1 of the proposed failure criterion for the dry shale samples

(b) Predicted σ_1 of the proposed failure criterion for the uniaxial compression condition of the shale samples with different moisture contents

(c) Predicted σ_1 of the proposed failure criterion for all the shale samples

(d) Predicted σ_1 of the Cai-Huang criterion for all the shale samples

(e) Predicted σ_1 of the modified Hoek–Brown criterion for the dry shale samples

(f) Predicted σ_1 of the Saeidi criterion for the dry shale samples

(g) Predicted σ_1 of the Al-Bazali criterion for the uniaxial compression condition of the shale samples with different moisture contents

Fig. 7. Comparisons of the predicted σ_1 for the failure criteria with the tested results.

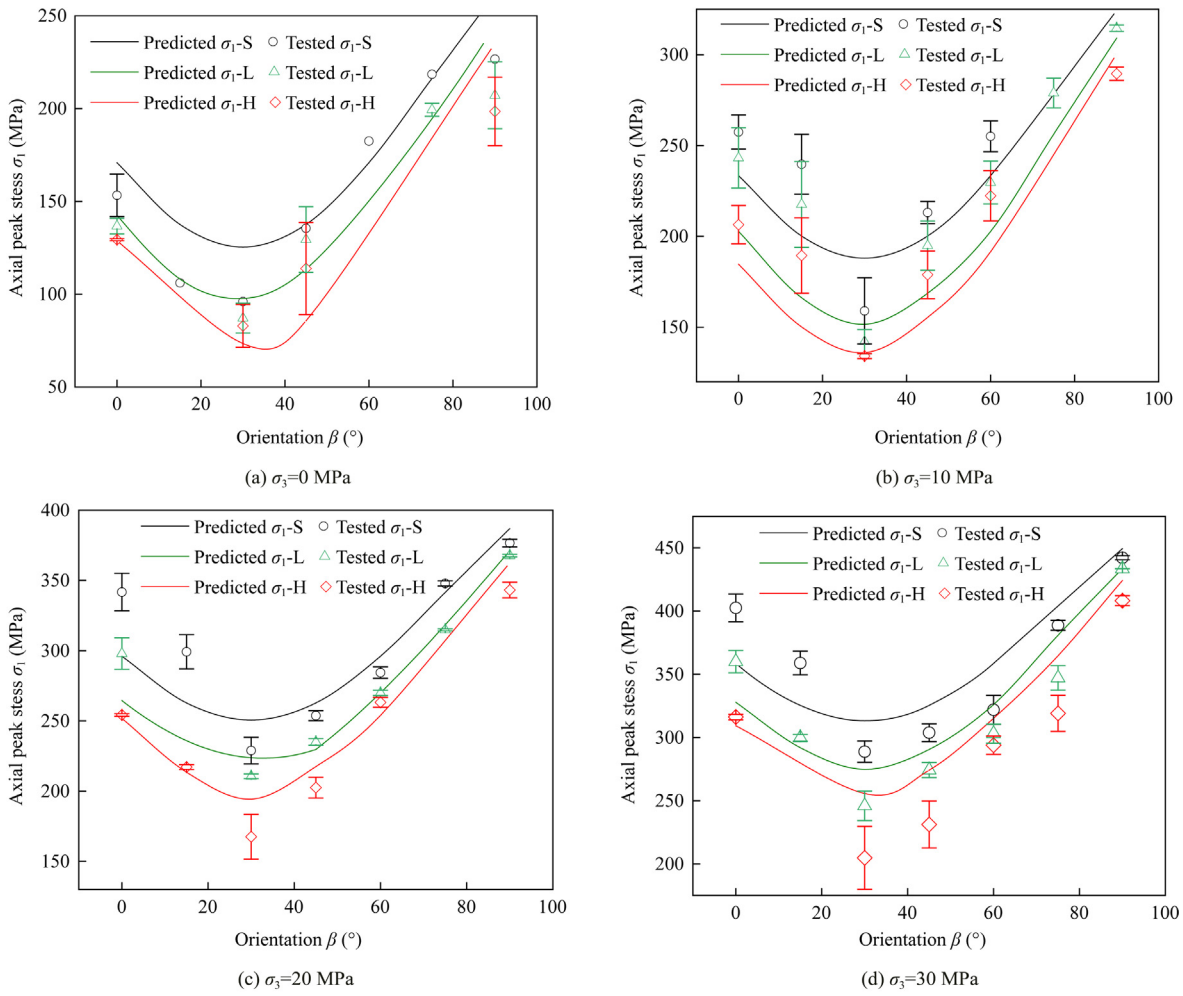

Fig. 8. Comparison between the predicted values of the proposed failure criterion and the tested results changed with β.

with k, as shown in Eq. (12). The absolute value of the changing rate is biggest for the shale sample at β=30°, certified by the changing rates of the predicted σ_1 with a 2.0 growth ratio of k, −16.354%, −24.170% and −6.404% for the shale samples at β=0°, 30° and 90°, respectively. This would be due to the effect of k on the predicted σ_1 that is multiplied by $\cos(\alpha-\beta)$, thus, considering that α=30°, the shale sample at β=30° will have a biggest changing rate of the predicted σ_1 with the increasing k. The absolute value of the changing rate rises with increasing ω_w, certified by the changing rates of the predicted σ_1 with a 2.0 growth ratio of k, −9.733 %, −16.173%, and −24.171% for the shale samples with ω_w=0.50%, 0.75%, and 1.00%, respectively. This can be explained by that the effect of k on the predicted σ_1 is multiplied by ω_w, for which a larger ω_w can cause a bigger changing rate of the predicted σ_1 with the increasing k. Therefore, the error of the predicted results will increase when the fitting accuracy of k becomes less, and this error increase would also increase for the shale sample when β is closer to 30° and ω_w becomes larger.

From Figs. 12 and 13, the predicted results are generally very sensitive to S_1, and are less sensitive to S_2 and k, but are very sensitive to S_2 at β=30°. From what has been discussed above, the accurate fitting parameters of S_1, S_2 and k can highly improve the prediction performance of the proposed failure criterion, and a lower predictive effect of the proposed failure criterion would be noted for the shale when β is closer to 30° and ω_w become higher, if the fitting accuracy of S_1, S_2 and k is poor.

4.7. Prediction performance of the proposed failure criterion with limited experimental data for parameters determination

A superior failure criterion is capable of predicting rock strength, even if the experimental data is limited to determine the model parameters [43]. In this failure criterion, the parameters of S_1, S_2, φ and k are determined by fitting the experimental data related to β, ω_w and σ_3. The other parameters of α, ω_{sh}, σ_s, d and l_0 are all determined by the independent methods. Therefore, the prediction performance of the proposed failure criterion is examined here considering four limited experimental data situations for parameters determination: (1) the experimental data of shale samples without available uniaxial compression test data; (2) the experimental data of shale samples without a specific β; (3) the available experimental data of shale samples at less β; (4) the experimental data of shale samples having limited moisture content level.

4.7.1. Prediction performance of the proposed failure criterion without available uniaxial compression test data for parameters determination

Fig. 14 shows the predicted σ_1 of the proposed failure criterion using the uniaxial and triaxial compression test data and only tri-

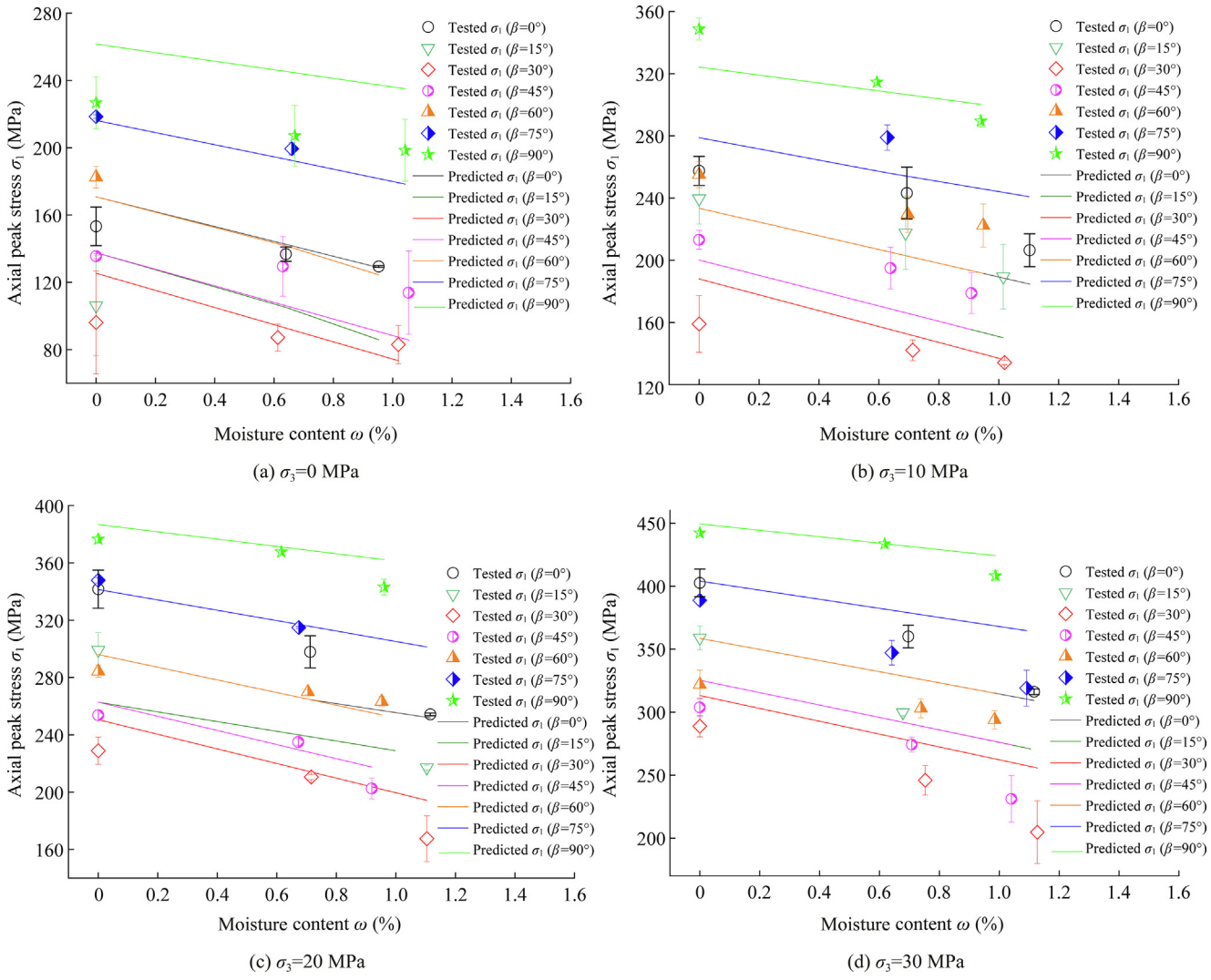

Fig. 9. Comparison between the predicted values of the proposed failure criterion and the tested results changed with moisture content.

axial compression test data for parameters determination compared with the tested σ_1. The values of S_1, S_2 and k are 41.499 MPa, 17.175 MPa and 5.118×10^{-4} for the first situation, and the values of S_1, S_2 and k are 40.439 MPa, 16.984 MPa and 5.720×10^{-4} for the second situation, showing a small difference between them. The error of the predicted σ_1 by the proposed failure criterion using the parameters determined by only triaxial compression test data is just a little higher than that using the parameters determined by the uniaxial and triaxial compression test data, as shown in Fig. 14. This indicates that the proposed failure criterion also has good prediction capability for the situation that the parameters are determined using only triaxial compression test data.

4.7.2. Prediction performance of the proposed failure criterion with the experimental data of shale samples without a specific β for parameters determination

In order to assess the contribution of the experimental data for the shale sample at each β on the predictive capability of the proposed failure criterion, an error analysis of the results is done here using the parameters determined by the experimental data of shale samples without a specific β. Since the experimental data of shale samples at β=90° should be used for determining φ, here the orientation β of 0°, 15°, 30°, 45°, 60°, and 75° for shale samples are used for analysis. The errors of the predicted σ_1 and the parameters (S_1, S_2, k) determined with the experimental data of shale samples without a specific β are presented in Table 5. According to the values of R^2 and AAREP in Table 5, we can clearly see that the error of the predicted σ_1 gradually increases with the data sets used for prediction without a β of 15°, 75°, 60°, 0°, 45° and 30°. However, all R^2 are higher than 0.91 and all AAREP are lower than 9.7 %, indicating that the prediction capability of this failure criterion is also excellent to use under these situations.

4.7.3. Prediction performance of the proposed failure criterion with available experimental data of shale samples at less β for parameters determination

The experimental data of the shale samples for less β are used to determine S_1, S_2 and k, and the corresponding errors of the predicted results are discussed here to analyze the prediction performance of the proposed failure criterion. The data set of the orientation β of the shale samples used for analysis is presented in Table 6. The errors of the results increase with the decrease in the number of β for the experimental data used for analysis. The error of that R^2 is higher than 0.91 and AAREP is lower than 9.4% for the predicted results using the experimental data of shale samples at β=0°, 30°, 45°, and 90° for parameters determination indicates that the predicted σ_1 agree well with the tested results

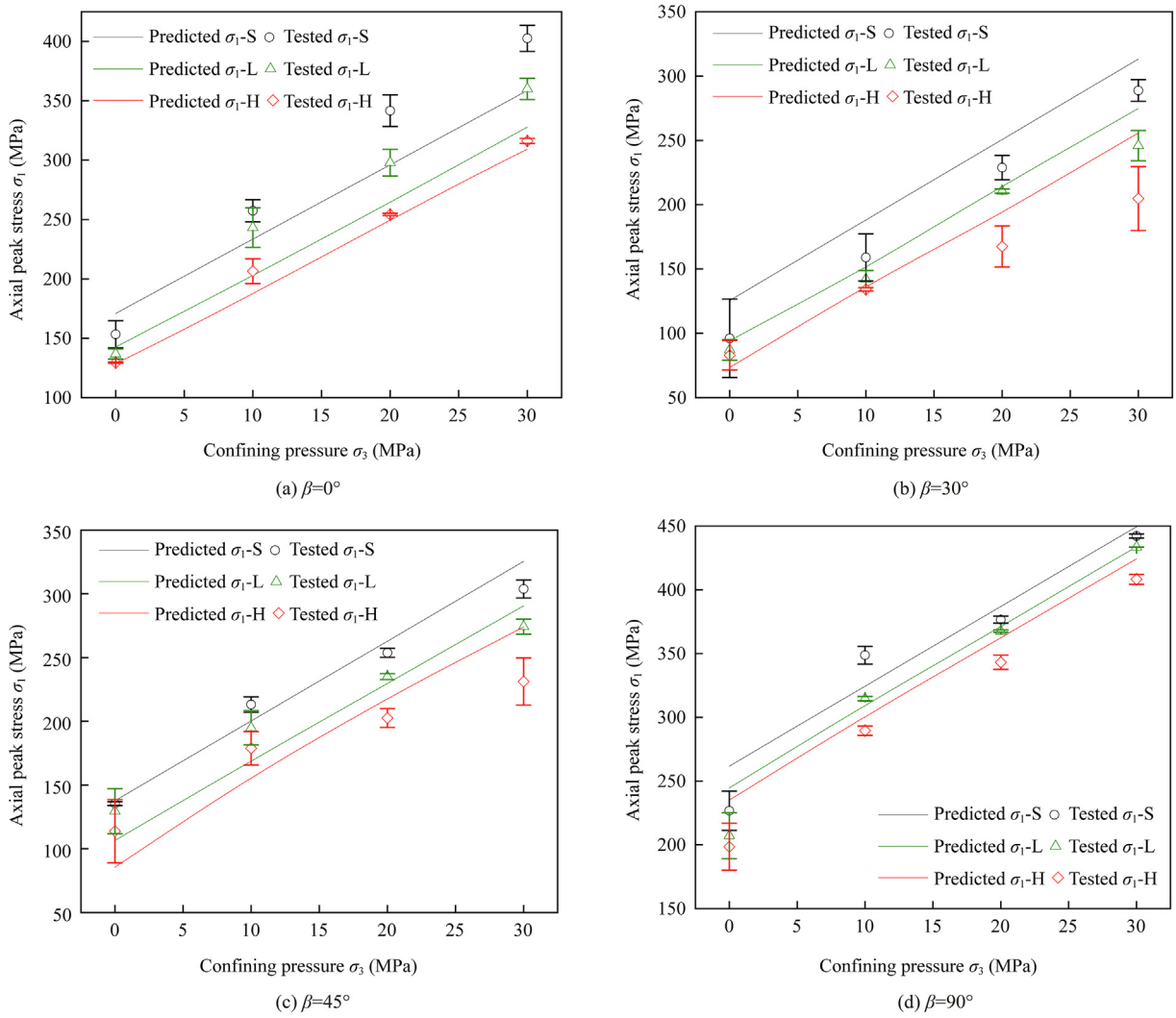

Fig. 10. Comparison between the predicted values of the proposed failure criterion and the tested results changed with confining pressure.

(Fig. 15). However, the error of the predicted σ_1 calculated by the parameters fitted with the experimental data of the shale samples at β=0°, 30°, and 90° shows that R^2 is lower than 0.9 and AAREP is bigger than 10%, as shown in Table 6. Therefore, a good prediction performance of the proposed failure criterion can be obtained if the parameters are determined with at least four β values (β=0°, 30°, 45°, and 90°).

4.7.4. Prediction performance of the proposed failure criterion with the experimental data of shale samples having limited moisture content level for parameters determination

The experimental data of S- and H-samples are used to determine k, and the error of the predicted results is discussed here. Table 7 presents the error of the predicted σ_1 and the parameters (S_1, S_2 and k) determined with the experimental data of shale sam-

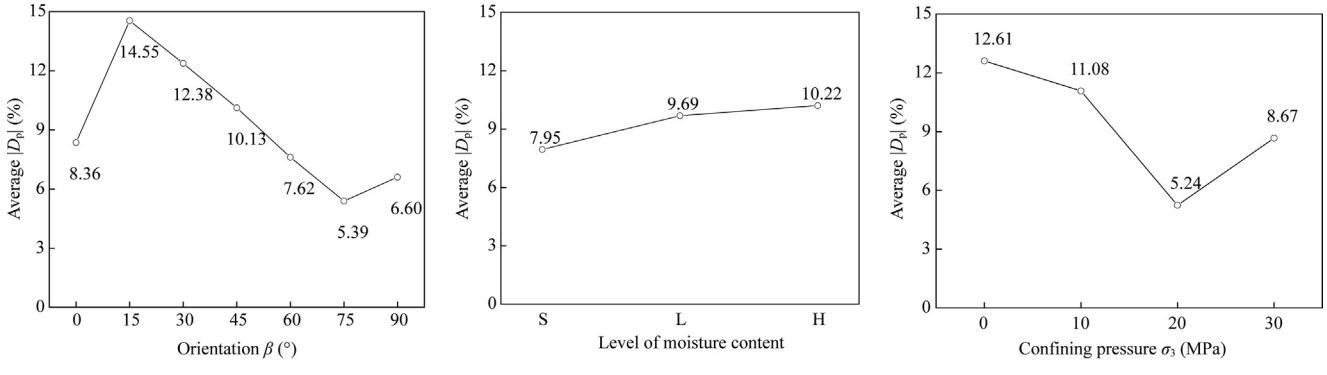

(a) With the change of orientation β (b) With the change of moisture content ω (c) With the change of confining pressure σ_3

Fig. 11. Error analysis of the predicted values of the proposed failure ceriterion compared with the tested results.

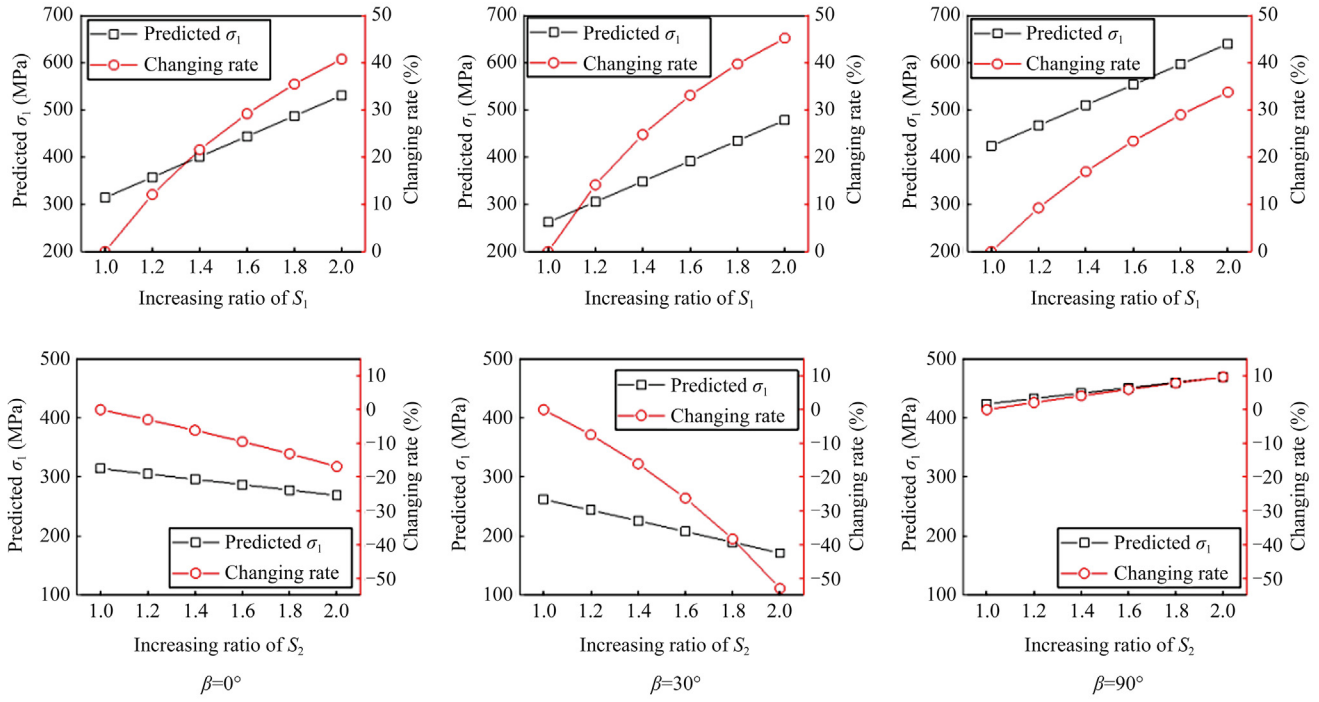

Fig. 12. Sensitivity analysis of S_1 and S_2 on the predicted σ_1 of the shale samples.

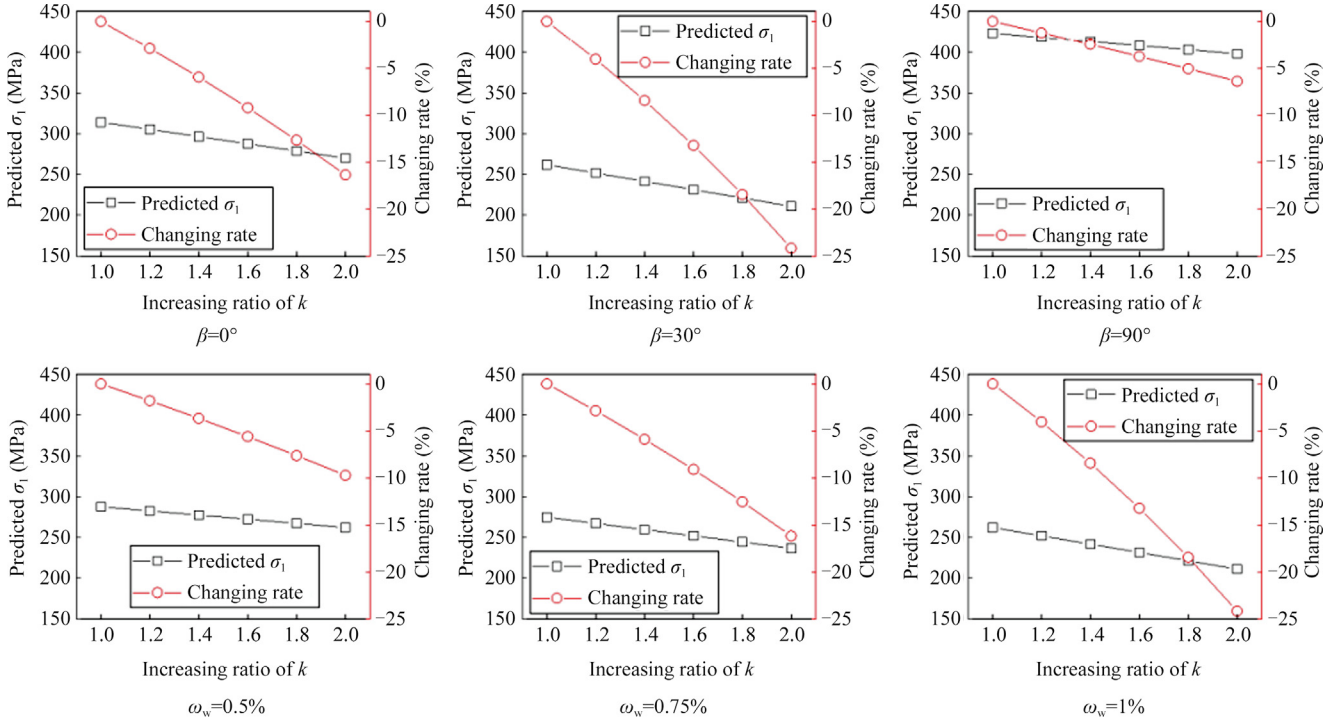

Fig. 13. Sensitivity analysis of k on the predicted σ_1 of the shale samples.

ples having different moisture content level sets. We can clearly find that the prediction performance of the proposed failure criterion is also excellent if the experimental data of S-samples and H-samples for seven β and the experimental data of S-, L-, and H-samples for four β are available for the parameter determination. Even the error of the results using the experimental data of S- and H-samples for four β can be accepted, which is verified by R^2 being greater than 0.9 and AAREP being lower than 9.7% for the predicted results.

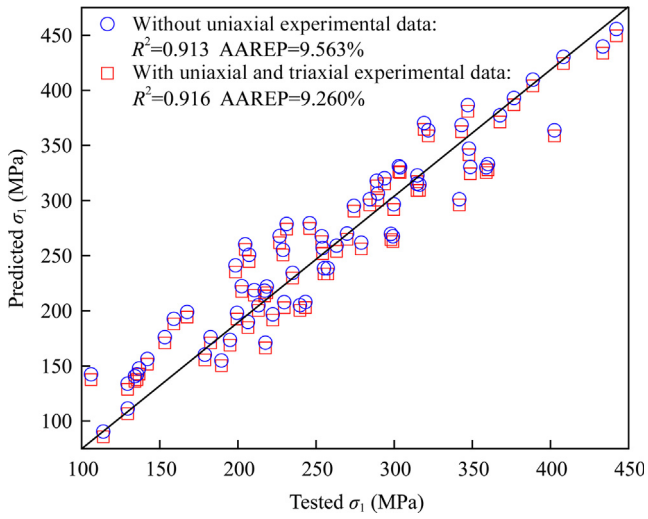

Fig. 14. Predicted σ_1 of the proposed failure criterion compared with the tested σ_1.

5. Discussions

As mentioned above, the proposed failure criterion has good prediction accuracy for the shale strength. The parameters of ω_{sh}, σ_s, d and l_0 are measured by the independent methods and the parameters of S_1, S_2, k and φ are fitted using the compression test results at least four β, with one level of moisture content. These model parameters have very clear physical meanings. There is only one new fitting parameter (k) in the proposed failure criterion besides the three fitting parameters (S_1, S_2 and φ) in Jaeger's shear failure criterion for transversely isotropic rocks, and all the fitting parameters are steady using the determination method. The evaluation of the proposed failure criterion shows excellent capability for the shale strength prediction.

The prediction accuracy of the proposed failure criterion depends on β, ω_w and σ_3 due to the concept of the shear slide failure model for rocks and the parameter determination method. When β is closer to 90° or 0°, more rock matrix sheets are cut by the shear failure plane according to the shear slide failure model, as shown in Fig. 2. The rock matrix sheets' failure has a small effect by water absorption [32]. The strength, when β is closer to 90° or 0°, can well be described by the proposed failure criterion. Additionally, φ is obtained by fitting the experimental data of the triaxial compression tests for the shale samples at β=90°, under different σ_3. Therefore, the prediction accuracy of the proposed failure criterion is better for the shale sample when β is closer to 90°, as shown in Figs. 8 and 11. On the other hand, since the bedding planes are subject to moisture and water action when the humidity environment changes and most microstructure changes occur along the inter-layers space, which can cause that the mechanical properties of shale becomes weaker when ω_w increases [44], the irregular change rule of the strength for the shale samples failed along bedding planes would become more sig-

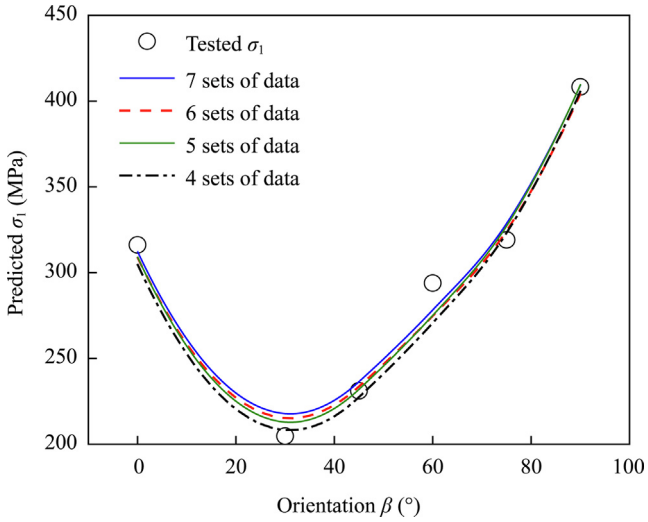

Fig. 15. Comparisons of the predicted σ_1 with the tested values using various sets of experimental data.

Table 5
Error of predicted σ_1 and parameters (S_1, S_2, k) determined with the experimental data of the shale samples for lacking a specific β.

Data sets	Orientation β of shale samples used for parameters determination (°)	Parameter			Error of the predicted σ_1	
		S_1	S_2	k	R^2	AAREP (%)
Data of shale samples without 0°	15, 30, 45, 60, 75, 90	39.689	17.050	5.598×10^{-4}	0.9135	9.2532
Data of shale samples without 15°	0, 30, 45, 60, 75, 90	40.487	16.707	5.955×10^{-4}	0.9163	9.3272
Data of shale samples without 30°	0, 15, 45, 60, 75, 90	40.253	18.069	5.512×10^{-4}	0.9105	9.3420
Data of shale samples without 45°	0, 15, 30, 60, 75, 90	40.449	14.820	5.865×10^{-4}	0.9136	9.6381
Data of shale samples without 60°	0, 15, 30, 45, 75, 90	40.557	16.971	5.916×10^{-4}	0.9156	9.3166
Data of shale samples without 75°	0, 15, 30, 45, 60, 90	40.549	17.093	5.572×10^{-4}	0.9153	9.2711

Table 6
Error of the predicted σ_1 and the parameters (S_1, S_2, k) determined with available experimental data of the shale samples for less β.

Orientation β of samples used for analysis (°)	Parameter			Error of the predicted σ_1	
	S_1	S_2	k	R^2	AAREP (%)
0, 15, 30, 45, 60, 75, 90	40.439	16.984	5.572×10^{-4}	0.9157	9.2602
0, 15, 30, 45, 60, 90	40.549	17.093	5.757×10^{-4}	0.9154	9.2798
0, 30, 45, 60, 90	40.313	18.126	5.328×10^{-4}	0.9107	9.2591
0, 30, 45, 90	40.315	18.125	5.482×10^{-4}	0.9104	9.3311
0, 30, 90	39.923	19.059	5.174×10^{-4}	0.8915	10.6496

Table 7
Error of predicted σ_1 and parameters (S_1, S_2, k) determined with available experimental data of the shale samples for limited moisture content level.

Orientation β of shale samples (°)	Moisture content level sets	Parameter			Error of the predicted σ_1	
		S_1	S_2	k	R^2	AAREP (%)
0, 15, 30, 45, 60, 75, 90	S, L, H	40.439	16.984	5.572×10^{-4}	0.9157	9.2602
0, 15, 30, 45, 60, 75, 90	S, H	40.439	16.984	6.225×10^{-4}	0.9147	9.4358
0, 30, 45, 90	S, L, H	40.315	18.125	5.482×10^{-4}	0.9104	9.3311
0, 30, 45, 90	S, H	40.315	18.125	6.062×10^{-4}	0.9076	9.6616

nificant with the increase in ω_w due to the differences in clay minerals content, pore structure and water action. This would result in that any failure criterion will predict the shale strength in a difficult manner. This is why the proposed failure criterion has a little low prediction accuracy for the strength of the shale sample at β=30° after water absorption, as mentioned in Section 4.5.2. In addition, σ_s is determined by the direct shear tests, for which condition the shear failure plane may not be the weakest plane of the shale sample after sufficient water absorption, as shown in Fig. 5b. In this case, the error of the predicted results would increase, even k is used to correct the effect of that. Therefore, the prediction accuracy decreases with the increasing ω_w, especially when β is closer to 30° due to the shear failure along the hydrated bedding planes, as shown in Figs. 9 and 11. Fortunately, confining stress will limit the effect of water absorption on the shale hydration [45], and the irregular change rule of the shale strength affected by the increase of ω_w will weaken with the increase in σ_3, resulting in the prediction accuracy being better under the condition of a higher σ_3 (Figs. 10 and 11).

The natural variability in the rock sample should be considered for estimating the accuracy of a failure criterion [46], and more experimental data used to fit the model parameters can increase the prediction accuracy. Although the prediction performance analysis, with limited experimental data, shows that the error of the results using the experimental data of S- and H-samples for four β can be accepted, as mentioned in Section 4.7.4, the obvious different errors for the different richness of the data can indicate that the abundant data for fitting the parameters can truly increase the prediction accuracy of the proposed failure criterion.

There are two limitations with respect to the proposed failure criterion based on the concept for developing it. On the one hand, the accuracy for predicting the strength of shale with tension failure may be unsatisfactory because this failure criterion is developed based on the shear slide failure model. The tension failure along the bedding planes will appear when the shale sample has low β and is tested under low σ_3 [26]. This can be verified by the change rule of the error for the shale sample at β=0° with σ_3, as shown in Fig. 8. On the other hand, the proposed failure criterion's good performance for predicting the hydration shale strength under high σ_3 needs to be further discussed. As shown in Eq. (12), the linear relation between σ_1 and σ_3 is determined in this failure criterion, which is in agreement with the results obtained by other scholars [47,48]. However, whether the linear relation between σ_1 and σ_3 can adapt for the shale sample tested under high σ_3 is worth thoroughly studying, because some scholars believe that the consideration of the parabolic relationship between σ_1 and σ_3 would be more reasonable for the rocks [49].

In general, the proposed failure criterion for hydration shale has a good prediction capability and clear physical meaning of the parameters and an easy parameter determination method. This failure criterion is intended for use in the strength prediction of hydration shale but can also be extended to other transversely isotropic rocks with the property of hydration. In addition, the engineering application to show the adaptability of the newly proposed failure criterion to evaluate the stability of geotechnical engineering structures in engineering practices need to be further discussed.

6. Conclusions

(1) On the basis of the shear slide failure model of rock, a novel failure criterion for hydration shale has been developed and presented. In this new failure criterion, Jaeger's shear failure criterion is used to describe shale's anisotropy. The effect of water on shale's strength considered in this failure criterion is based on the fact that the strength of the shear failure plane with respect to β in shale would decrease resulting from clay minerals hydration. This shear strength decrease is determined by the geometrical relationship between the hydrated clay minerals layers and the shear failure plane. When the effect of water is not taken into account (ω_w=0), the proposed failure criterion becomes Jaeger's shear failure criterion.

(2) The newly proposed failure criterion consists of nine parameters. They are four parameters in Jaeger's shear failure criterion (S_1, S_2, α and φ), three hydration parameters of shale (k, ω_{sh}, and σ_s), and two material size parameters (d and l_0). The physical meanings of these parameters and procedures for determining these parameters are described.

(3) The accuracy and applicability of the proposed failure criterion are examined using the published experimental data, showing a good agreement between the predicted values and the testing results, which can be verified by R^2=0.916 and AAREP=9.260%. Also, the prediction performance of the proposed failure criterion is demonstrated to have a better prediction performance compared with other four failure criteria.

(4) The errors ($|D_p|$) of the predicted values are analyzed considering the effects of β (angle between bedding plane versus axial loading), moisture content (ω_w), and confining pressure (σ_3). The results show that $|D_p|$ increases when β is closer to 30°, and $|D_p|$ increases with the increasing ω_w, but $|D_p|$ decreases with the increase in σ_3.

(5) The parameter sensitivity of the proposed failure criterion is also presented, showing that the predicted values are sensitive to S_1, and less sensitive to S_2 and k, but very sensitive to S_2 at β=30°. The accurate fitting parameters of S_1, S_2 and k can highly improve the prediction performance of the proposed failure criterion, but a lower predictive effect should be noted when β is closer to 30° and for shale sample with a higher ω_w.

(6) The prediction performance of the proposed failure criterion with the limited data set for parameters determination is discussed, showing that good accuracy can be acquired by determining the parameters using the compression tests data of shale samples with at least four β values (β=0°, 30°, 45° and 90°). Even, the prediction values with the experimental data of the shale samples for the four β and with only one level of moisture content has the accepted error.

(7) The proposed failure criterion can be employed to evaluate the shale strength considering the anisotropy and hydration of shale, together with some physical experiments and compression tests of shale. Meanwhile, this failure criterion can also be extended to the strength prediction for other transversely isotropic rocks with the property of hydration.

Acknowledgements

The financial supports from the Sichuan Science and Technology Program (No. 2022NSFSC0185), the National Natural Science Foundation of China (Nos. 42172313 and 51774246), the Natural Science Foundation of Chongqing (No. cstc2020jcyj-msxmX0570), the Fundamental Research Funds for the Central Universities (Nos. 2020CDJ-LHZZ-004, 2020CDJQY-A046), and the State Key Laboratory of Coal Mine Disaster Dynamics and Control (No. 2011DA105287-MS201903) are appreciated. The scholarship supports provided by the China Scholarship Council (CSC) is gratefully acknowledged. The authors would like to express their gratitude to the editors and anonymous reviewers for their constructive comments on the draft paper.

References

[1] Shen JY, Karakus M. Three-dimensional numerical analysis for rock slope stability using shear strength reduction method. Can Geotech J 2014;51(2):164–72.
[2] Fan XY, Zhang MM, Zhang QG, Zhao PF, Yao BW, Lv D. Wellbore stability and failure regions analysis of shale formation accounting for weak bedding planes in Ordos basin. J Nat Gas Sci Eng 2020;77:103258.
[3] Shi H, Song L, Zhang HQ, Chen WL, Lin HS, Li DQ, Wang GZ, Zhao HY. Experimental and numerical studies on progressive debonding of grouted rock bolts. Int J Min Sci Technol 2022;32(1):63–74.
[4] Kamali-Asl A, Ghazanfari E, Newell P, Stevens M. Elastic, viscoelastic, and strength properties of Marcellus Shale specimens. J Petroleum Sci Eng 2018;171:662–79.
[5] Hu YL, Shi XC, Li QL, Gao LY, Wu F, Xie G. Effects of a polyamine inhibitor on the microstructure and macromechanical properties of hydrated shale. Petroleum 2022;8(1):1–10.
[6] He PF, Kulatilake PHSW, Yang XX, Liu DQ, He MC. Detailed comparison of nine intact rock failure criteria using polyaxial intact coal strength data obtained through PFC3D simulations. Acta Geotech 2018;13(2):419–45.
[7] Xie HP, Lu J, Li CB, Li MH, Gao MZ. Experimental study on the mechanical and failure behaviors of deep rock subjected to true triaxial stress: A review. Int J Min Sci Technol 2022;32(5):915–50.
[8] Li B, Liu J, Bian K, Ai F, Hu X, Chen M, Liu Z. Experimental study on the mechanical properties weakening mechanism of siltstone with different water content. Arab J Geosci 2019;12(21):1–14.
[9] Yao QL, Tang CJ, Xia Z, Liu XL, Zhu L, Chong ZH, Hui XD. Mechanisms of failure in coal samples from underground water reservoir. Eng Geol 2020;267:105494.
[10] Lashkaripour GR, Passaris EKS. In: Correlations between index parameters and mechanical properties of shales. Tokyo: International Society for Rock Mechanics; 1995. p. 257–61.
[11] Al-Bazali T. The impact of water content and ionic diffusion on the uniaxial compressive strength of shale. Egypt J Petroleum 2013;22(2):249–60.
[12] Huang RZ, Chen M, Deng JG, Wang KP, Chen ZX. Study on shale stability of wellbore by mechanics coupling with chemistry method. Driuing Fluid Complet Fluld 1995(3):. 15–21. in Chinese.
[13] Li DY, Wong LNY, Liu G, Zhang XP. Influence of water content and anisotropy on the strength and deformability of low porosity meta-sedimentary rocks under triaxial compression. Eng Geol 2012;126:46–66.
[14] Chong ZH, Li XH, Hou P, Chen XY, Wu YC. Moment tensor analysis of transversely isotropic shale based on the discrete element method. Int J Min Sci Technol 2017;27(3):507–15.
[15] Gao ZW, Zhao JD, Yao YP. A generalized anisotropic failure criterion for geomaterials. Int J Solids Struct 2010;47(22–23):3166–85.
[16] Pietruszczak S, Mroz Z. On failure criteria for anisotropic cohesive-frictional materials. Int J Numer Anal Meth Geomech 2001;25(5):509–24.
[17] Jaeger JC. Shear failure of anistropic rocks. Geol Mag 1960;97(1):65–72.
[18] Donath FA. Experimental study of shear failure in anisotropic rocks. Geol Soc America Bull 1961;72(6):985.
[19] Yin PF, Yang SQ. Experimental study on strength and failure behavior of transversely isotropic rock-like material under uniaxial compression. Geomech Geophys Geo Energy Geo Resour 2020;6(3):1–19.
[20] Saroglou H, Tsiambaos G. A modified Hoek-Brown failure criterion for anisotropic intact rock. Int J Rock Mech Min Sci 2008;45(2):223–34.
[21] Zhang QG, Yao BW, Fan XY, Li Y, Li MH, Zeng FT, Zhao PF. A modified Hoek-Brown failure criterion for unsaturated intact shale considering the effects of anisotropy and hydration. Eng Fract Mech 2021;241:107369.
[22] Hoek E, Brown ET. The Hoek-Brown failure criterion and GSI - 2018 edition. J Rock Mech Geotech Eng 2019;11(3):445–63.
[23] Pei JY, Einstein HH, Whittle AJ. The normal stress space and its application to constructing a new failure criterion for cross-anisotropic geomaterials. Int J Rock Mech Min Sci 2018;106:364–73.
[24] Pietruszczak S, Mroz Z. Formulation of anisotropic failure criteria incorporating a microstructure tensor. Comput Geotech 2000;26(2):105–12.
[25] Chen M, Jin Y, Zhang G. Petroleum Engineering Rock Mechanics. Beijing: Science Press; 2008. p. 23. in Chinese.
[26] Niandou H, Shao JF, Henry JP, Fourmaintraux D. Laboratory investigation of the mechanical behaviour of Tournemire shale. Int J Rock Mech Min Sci 1997;34(1):3–16.
[27] Kang YL, Yang B, Li XC, Yang J, You LJ, Chen Q. Quantitative characterization of micro forces in shale hydration and field applications. Petroleum Explor Dev 2017;44(2):328–35.
[28] Pashley RM. DLVO and hydration forces between mica surfaces in Li^+, Na^+, K^+, and Cs^+ electrolyte solutions: A correlation of double-layer and hydration forces with surface cation exchange properties. J Colloid Interface Sci 1981;83(2):531–46.
[29] Fan XY, Guo DY, Zhang QG, Xu FL, Liang YC, Lu XW, Ni T. Experimental study on the crack propagation mechanism of shale considering the effect of the bedding, loading rate and sample size. Sci Technol Eng 2018;18(9):63–71. in Chinese.
[30] Yao QL, Li XH, Zhou J, Ju MH, Chong ZH, Zhao B. Experimental study of strength characteristics of coal specimens after water intrusion. Arab J Geosci 2015;8(9):6779–89.
[31] Hu KF, Feng Q, Wang XT. Experimental research on mechanical property of phyllite tunnel surrounding rock under different moisture state. Geotech Geol Eng 2017;35(1):303–11.
[32] Zhang QG, Fan XY, Chen P, Ma TS, Zeng FT. Geomechanical behaviors of shale after water absorption considering the combined effect of anisotropy and hydration. Eng Geol 2020;269:105547.
[33] Zhang QG, Wang LZ, Zhao PF, Fan XY, Zeng FT, Yao BW, He L, Yang SM, Feng Y. Mechanical properties of lamellar shale considering the effect of rock structure and hydration from macroscopic and microscopic points of view. Appl Sci 2022;12(3):1026.
[34] Ma TS, Yang CH, Chen P, Wang XD, Guo YT. On the damage constitutive model for hydrated shale using CT scanning technology. J Nat Gas Sci Eng 2016;28:204–14.
[35] Wang H, Li Y, Cao SG, Fantuzzi N, Pan RK, Tian MY, Liu YB, Yang HY. Fracture toughness analysis of HCCD specimens of Longmaxi shale subjected to mixed mode I-II loading. Eng Fract Mech 2020;239:107299.
[36] Cai MF, He MC, Liu DY. Rock Mechanics and Engineering. Beijing: Science Press; 2002. p. 104–108. in Chinese.
[37] Rafiai H. New empirical polyaxial criterion for rock strength. Int J Rock Mech Min Sci 2011;48(6):922–31.
[38] Saeidi O, Rasouli V, Vaneghi RG, Gholami R, Torabi SR. A modified failure criterion for transversely isotropic rocks. Geosci Front 2014;5(2):215–25.
[39] Shen JY, Karakus M. Simplified method for estimating the Hoek-Brown constant for intact rocks. J Geotech Geoenviron Eng 2014;140(6):971–84.
[40] Bonnelye A, Schubnel A, David C, Henry P, Guglielmi Y, Gout C, Fauchille AL, Dick P. Strength anisotropy of shales deformed under uppermost crustal conditions. J Geophys Res Solid Earth 2017;122(1):110–29.
[41] Wang MM, Li P, Wu XW, Xu D. Analysis of the stress ratio of anisotropic rocks in uniaxial tests. Int J Min Sci Technol 2017;27(3):531–5.
[42] Ma TS, Chen P. A wellbore stability analysis model with chemical-mechanical coupling for shale gas reservoirs. J Nat Gas Sci Eng 2015;26:72–98.
[43] Wang DJ, Tang HM, Shen PW, Cai Y. A parabolic failure criterion for transversely isotropic rock: Modification and verification. Math Probl Eng 2019;2019:8052560.
[44] Minaeian V, Dewhurst DN, Rasouli V. Deformational behaviour of a clay-rich shale with variable water saturation under true triaxial stress conditions. Geomech Energy Environ 2017;11:1–13.
[45] Al-Mhaidib AI. Swelling behaviour of expansive shales from the middle region of Saudi Arabia. Geotech & Geol Eng 1998;16:291–307.
[46] Das SK, Basudhar PK. Comparison of intact rock failure criteria using various statistical methods. Acta Geotech 2009;4(3):223–31.
[47] Cabezas R, Vallejos J. Nonlinear criterion for strength mobilization in brittle failure of rock and its extension to the tunnel scale. Int J Min Sci Technol 2022;32(4):685–705.
[48] Wu XZ, Jiang YJ, Guan ZC. A modified strain-softening model with multi-post-peak behaviours and its application in circular tunnel. Eng Geol 2018;240:21–33.
[49] Eberhardt E. The Hoek-Brown failure criterion. Rock Mech Rock Eng 2012;45(6):981–8.